論 文
36~12~5

마이크로 컴퓨터를 이용한 동기전동기의 최대 효율제어

Microcomputer-Based Maximum Efficiency Control of a Synchronous Motor.

玄 東 石*·朴 旻 鎬**
(Dong-Seok Hyun · Min-Ho Park)

요 약

本 研究에서는 임의의 어떤 특정한 토오크 및 速度에서 항상 最大效率로 定常運轉될 수 있도록 界磁, 電機子 電壓 및 負荷角을 最適値로 制御하여 실질적인 同期電動機의 效率向上을 成就할 수 있었으며 또한 力率도 改善 制御될 수 있는 附加的인 效果도 가져올 수 있었다. 특히 輕負荷 運轉時에서는 效率向上과 力率改善이 顯著하였다.

이상과 같은 解析를 위하여 周波數에 따른 電動機의 파라미터 및 鐵損에 대한 影響을 考慮한 보다 正確하고 合理的인 等價回路 모델을 構成하여 보다 實際에 부합케 하였다.

이와 같은 最適效率 運轉時 系統의 安定度를 判別하기 위하여 定常運轉 狀態로부터 微小變化에 따른 運動機 特性을 갖는 線型化된 方程式을 誘導하여 Nyquist 安定度判別法을 適用하여 그 結果를 提示하였다.

그리고 同期電動機의 高調波 損失 및 토오크 脈動分을 보다 減少시키기 위하여 制御 루우프로 16비트 마이크로 컴퓨터와 電力回路로 펄스 크기조정 인버어터를 使用하여 實際 驅動시스템을 具現하였다. 이와 같은 시스템은 消弧角을 위한 메모리를 대폭적으로 줄일 수 있었고 制御 알고리즘의 단순화를 기할 수 있었다.

ABSTRACT

The efficiency of a synchronous motor can be substantially improved by controlling armature voltage, field excitation, and load angle on optimun values which yield minimum input power at any specified torque and speed. This improvement is particularly noticeable in the case of light loads. In addition, the control of armature input voltage improves the power factor at which the motor operates.

Employed in the analysis is a new equivalent circuit model of the motor which incorporates the frequency dependent nature of the motor parameters and the effects of iron loss.

The stability of synchronous motor operation is studied by applying the Nyquist stability criterion to the linearized equations which describe the behavior of the motor as the motor loads perturb about a steady-state operating point. This investigation reveals that, in some cases, the stable region of the motor is delineated from the results of a computer simulation.

With a view to reducing harmonic loss and improving torque pulsation from harmonic components, a very poweful pulse amplitude modulation (PAM) method using an 16-bit microcomputer has been developed. This method has the advantages of simplicity of control algorithms and requires small memory space for storing thyristor trigger angles for a three-phase PAM inverter. The method can be used for smooth control of both modulation depth and frequency over a wide range.

Ⅰ. INTRODUCTION

A recent study by the U.S. Department of Energy noted that electric energy consists of about 40% of all the energy generated and that 60 to 70% of all the electric energy is consumed by electric motor driven systems[1) 2)]. From this fact it is evident that the electric motor driven systems, if and when improved, will save considerable energy since operating cost saving accrued by efficiency optimized operation is considered to be substantial in the life cycle of drive systems.

Synchronous motors are particuarly economical from the standpoint of cost and efficency when low speed is applied with direct connected loads (without reduction gears), such as compressors, grinders, and mixers, especially in ratings of 100 hp or more. At these low speed ratings, the synchronous motor is less expensive than an induction motor of the same rating. With the additional advantage of being a source of reactive power, the motor is capable of meeting larger peak loads in such devices as ball-mills and crusher[3)-8)]. Besides, it can keep a constant desired speed under frequent load disturbances. In this dissertation, an effort is made to define an optimum condition yielding maximum efficiency and good power factor in the stable region at any specified torque and speed in a variable frequency driven system: to present the control with stability analysis of the motor driven system with maximum efficincy.

In order to achieve this task, it is essential first to develop an equivalent circuit model that may be used to make sufficiently accurate predictions about motor performance and characteristics with iron loss component. A new equivalent circuit model may easily be developed by focusing on the characterization of the magnetic field interactions occurring along the zero, direct, and quadrature axes of the synchronous motor.

A new equivalent circuit model may be derived from that of an induction machine[7)-9)]. In the induction mode of operation, the secondary frequency, which is a variable, is determined by the relative motion of the air gap field and the secondary windings. The same machine can be made to operate in the synchronous mode wherein the secondary voltage is no longer produced by induction, but is provided by an external sypply, normally direct current, which determines the frequency of this winding voltage.

If the induction machine were to rate at synchronous speed, as is widely known, there would be no induced voltage because the secondary windings would be at rest with respect to the movig field. If a dc current were to be applied to the secondary, however, a steady field pattern would be established, which would lock in synchronism with the primary field moving at the same speed[19) 20)].

Consequently, when both primary and secondary windings carry curent, each yields leakage flux and mutual flux. In other words, each mmf can be considered as producing its own flux, some of which are leakages and the rest of which are two mutual compoents of effective flux crossing the airgap, which can be combined vectorially to give the same resultant mutual flux. Thus, the only resultant mutual flux affects the effective core loss of the synchronous machine[10)].

Based on this and by applying Lagrange multiplier theory to a nonlinear equation derived from the new equivalent circuit model, an optimum condition can be established precisely to maximize efficiency of a synchronous motor. As efficiency improvement of the motor is dependent upon air gap flux, which is a function of field excitation, armature voltage, and armature current, motor efficiency can be improved by means of optimized control of field excitation and armature voltage at any specified load.

This energy saving measure, particularly fixed frequency synchronous motor drives, has recently received considerable publicity[11)]. This control is also appropriate for variable frequency drive systems that can now supply variable frequency power to accomplish the predicted frequency changes thanks to recent advances in power semiconductior technology.

In a variable frequency synchronous motor drive, a specified torque-speed operating point can be achieved with a variety of field excitation and armature voltage combinations as shown in Fig. 1-1. Therefore, the motor efficiency may vary widely, but armature voltage is usually maintained at its nominal value while field ex-

*正 會 員：漢陽大工大電氣工學科 副教授・工博
**正 會 員：서울大工大電氣工學科 教授・工博
接受日字：1987年 9月 17日
1次修正：1987年 11月 17日
2次修正：1987年 12月 5日

citation normally keeps the value of 1.0 or 0.8 power factor by conventional control strategy.

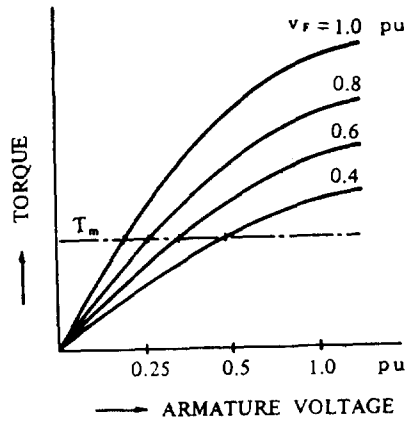

Fig. 1-1. Torque vs. armature voltage for each field voltage (v_F).

In this strategy, there is an excessive core loss due to air-gap flux, particularly at lighted loads. Accordingly, the motor efficiency can be significantly improved by adjusting the air gap flux to the optimum value: there is an optimum field excitation and armature voltage combination to yield maximum efficiency at any specified load[12) 13)]. The algorithm is realized by a 16-bit microcomputer, control circuits, and power circuits.

To investigate the feasibility of the synchronous motor as a variable speed device, it is important to establish a set of equations which permits an analysis of motor stability at any speed. Studies of free oscillation or instability of the synchronous motor have been conducted, but the approximations made in these investigations are not applicable at low frequencies[13) 14)].

Equations describing the behavior of the synchronous motor for small excursions about a steady state operating point are developed using the method of small displacements. A stability analysis is then performed by employing the Nyquist stability criterion[15)16)]. The effect of varying the field excitation and amplitude of the armature voltage is discussed in some detail. This study reveals that the synchronous motor is lightly damped and may even be unstable at low speed[17) 18)].

Ⅱ. MATHEMATICAL DESCRIPTION

The assumptions on which the model and the present analysis are based are listed below:

1) The stator windings are sinusoidally distributed around the periphery along the air gap as far as all mutual with the rotor are concerned.
2) The effect of the stator on the variation of any of the rotor inductances with rotor angle is not considered.

The synchronous machine under consideration is assumed to have three stator windings, one field winding, and two amortisseur windings. These six windings are magnetically coupled. The magnetic coupling between windings is a function of rotor position. Thus the flux linking each winding is also a function of rotor position. Thus the flux linking each winding is also a function of rotor position. The instantaneous terminal voltage v of any winding is in the form:

$$v = \pm\sum ri \pm \sum \dot{\lambda} \text{[pu]} \qquad (2-1)$$

where λ is flux linkage, r winding resistance, and i current, with direcitonally positive stator current flowing into the machine terminals. The notation $\pm\sum$ indicates the summation of all appropriate terms with due regard to signs. The expressions for winding voltages are complicated because of the variation of λ with the rotor position. Thus in voltage equations such as eq. (2-1) the $\dot{\lambda}$ term is not a simple Li but must be computed as $\dot{\lambda}=L\dot{i}+\dot{L}i$.

The voltage equations of a synchronous machine are in the form of eq. (2-1). Schematically, circuits are shown in Fig. 2-1. Mutual inductances are omitted from the schematic for clarity but are assumed to be present with the values given in flux linkage equations. In the case of a motor the voltage equation for the conditions indicated is as follows[21)]:

$$\begin{bmatrix} v_{abc} \\ v_{FDQ} \end{bmatrix} = \begin{bmatrix} R_{abc} & 0 \\ 0 & R_{FDQ} \end{bmatrix} \begin{bmatrix} i_{abc} \\ i_{FDQ} \end{bmatrix} + \begin{bmatrix} \lambda_{abc} \\ \lambda_{FDQ} \end{bmatrix} + \begin{bmatrix} v_n \\ 0 \end{bmatrix} \text{[pu]} \qquad (2-2)$$

where

$v_{abc} = [v_a \ v_b \ v_c]^T$

$v_{FDQ} = [v_F \ v_D \ v_Q]^T$

$R_{abc} = [r_a \ r_b \ r_c]^T$

$R_{FDQ} = [r_F \ r_D \ r_Q]^T$

$$i_{abc}=[i_a\ i_b\ i_c]^T$$
$$i_{FDQ}=[i_F\ i_D\ i_Q]^T$$
$$\lambda_{abc}=[\lambda_a\ \lambda_b\ \lambda_c]^T$$
$$\lambda_{FDQ}=[\lambda_F\ \lambda_D\ \lambda_Q]^T$$
$$v_n=r_n\begin{bmatrix}1&1&1\\1&1&1\\1&1&1\end{bmatrix}\begin{bmatrix}i_a\\i_b\\i_c\end{bmatrix}+L_n\begin{bmatrix}1&1&1\\1&1&1\\1&1&1\end{bmatrix}\begin{bmatrix}\dot{i}_a\\\dot{i}_b\\\dot{i}_c\end{bmatrix}$$
$$=R_n i_{abc}+L_n\dot{i}_{abc}\ [\mathrm{pu}]$$

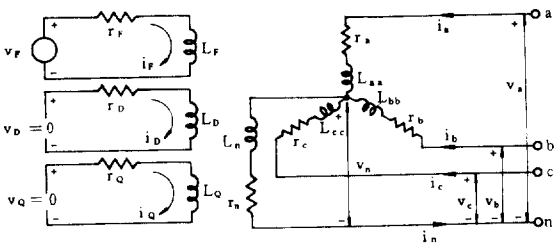

Fig. 2-1. Schematic diagram of a synchronous machine.

Thus eq. (2-2) is complicated by the presence of time-varying coefficients in $\dot{\lambda}$ term, but these terms can be eliminated by applying Park's transformation to the stator partition. This requires that both sides of eq. (2-2) be premultiplied by $\begin{bmatrix}P&0\\0&U_3\end{bmatrix}$.

$$\begin{bmatrix}v_{odq}\\v_{FDR}\end{bmatrix}=\begin{bmatrix}R_{abc}&0\\0&R_{FDQ}\end{bmatrix}\begin{bmatrix}i_{odq}\\i_{FDQ}\end{bmatrix}+\begin{bmatrix}\lambda_{odq}\\\lambda_{FDQ}\end{bmatrix}$$
$$-\begin{bmatrix}\dot{P}P^{-1}\ \lambda_{odq}\\0\end{bmatrix}+\begin{bmatrix}n_{odq}\\0\end{bmatrix}[\mathrm{pu}]\qquad(2-3)$$

where

$$P=\sqrt{2/3}\begin{bmatrix}\sqrt{1/2}&\sqrt{1/2}&\sqrt{1/2}\\\cos\theta&\cos(\theta-2\pi/3)&\cos(\theta+2\pi/3)\\-\sin\theta&-\sin(\theta-2\pi/3)&-\sin(\theta+2\pi/3)\end{bmatrix}$$

$$n_{odq}=Pv_n=PR_nP^{-1}Pi_{abc}+PL_nP^{-1}Pi_{abc}$$
$$=\begin{bmatrix}3r_ni_o\\0\\0\end{bmatrix}+\begin{bmatrix}3L_n\dot{i}_o\\0\\0\end{bmatrix}[\mathrm{pu}]$$

All terms in this equation are known, The resistace matrix is diagonal. In eq. (2-3), replacing the terms in λ and $\dot{\lambda}$ by terms in i and $\dot{i}$

A great deal of information is contained in eq. (2-4). First, the zero-sequence voltage is dependent only upon

$$\begin{bmatrix}v_o\\v_d\\v_F\\v_D=0\\v_q\\v_Q=0\end{bmatrix}=\begin{bmatrix}r+3r_n&0&0&0&0&0\\0&r&0&0&-\omega L_q&-\omega kM_Q\\0&0&r&0&0&0\\0&0&0&r_D&0&0\\0&\omega L_d&\omega kM_F&\omega kM_D&r&0\\0&0&0&0&0&r_Q\end{bmatrix}\begin{bmatrix}i_o\\i_d\\i_F\\i_D\\i_q\\i_Q\end{bmatrix}$$
$$+\begin{bmatrix}L_0+3L_n&0&0&0&0&0\\0&L_d&kM_F&kM_D&0&0\\0&kM_F&L_F&M_R&0&0\\0&kM_D&M_R&L_D&0&0\\0&0&0&0&L_Q&r\\0&0&0&0&kM_Q&L_Q\end{bmatrix}\begin{bmatrix}\dot{i}_o\\\dot{i}_d\\\dot{i}_F\\\dot{i}_D\\\dot{i}_q\\\dot{i}_Q\end{bmatrix}[\mathrm{pu}]\qquad(2-4)$$

i_0 and $\dot{i}_0$. This equation can be solved separately from the others once the initial conditions on i_0 are given. The remaining five equations are all coupled in a most interesting way. They are similar to those of a passive network except for the presence of the speed voltage terms. These terms, cosisting of $\omega\lambda$ or ωLi products, appear asymmetrical and distinguish this equation from that of a passive network. The speed voltage terms in the d-axis equation are due only to q-axis currents, viz., i_q and i_Q. Similarly, the q-axis speed voltages are due to d-axis currents, i_d, i_F, and i_D. Also all the terms in the coefficient matrices are constants except ω, the angular velocity. This is a considerable improvement over the description given in eq. (2-2) in the a-b-c frame of reference since nearly all inductances in that equation were time varing. since ω is a variable, this causes eq. (2-4) to be nonlinear. If the speed is assumed constant, which is usually a good approximation, then eq. (2-4) is linear. In any event, the nonlinearity is never great, as ω is usually nearly constant. But iron loss terms that are inevitably proposed for efficiency problems are not contained in eq. (2-4). Consequently, as already presented by authors[22], a new equivalent circuit of synchronous machine can be realized by putting the iron loss term in the conventional equivalent circuit. As iron loss is a function of induced (back) electromotive force, or just emf, it is very improtant to define the induced electromotive force in the elertric machnie[4] [8]. According to Faraday's law, the emf can conveniently be resolved into two terms: the time variation of the air-gap magnetic field and the relative motion of stator with respect to the reference coordinate frame in which the magnetic

field is specified. Accordingly, as a induction machine, if a imaginary resistance corresponding to iron loss can be considered as shown in Fig. 2-2, the voltage equations of the d-axis circuits under balanced conditions are:

$$v_d = r(i_d+i_{od}) + \ell_d(\dot{i}_d+\dot{i}_{od}) + L_{AD}(\dot{i}_d+\dot{i}_F+\dot{i}_D) - \omega L_{AQ}(i_q+i_Q) - \omega\ell_q(i_q+i_{oq}) \quad [pu] \qquad (2-5)$$

$$v_F = r_F i_F + \ell_F \dot{i}_F + L_{AD}(\dot{i}_d+\dot{i}_F+\dot{i}_D) \quad [pu] \qquad (2-6)$$

$$v_D = 0 = r_D i_D + L_{AD}(\dot{i}_d+\dot{i}_F+\dot{i}_D) \quad [pu] \qquad (2-7)$$

Similarly, for q-axis circuits:

$$v_q = r(i_q+i_{oq}) + \ell_q(\dot{i}_q+\dot{i}_{oq}) - L_{AQ}(\dot{i}_q+\dot{i}_Q) + \omega L_{AD}(i_d+i_F+i_D) + \omega\ell_d(i_d+i_{od}) \quad [pu] \qquad (2-8)$$

$$v_Q = r_Q i_Q + \ell_Q \dot{i}_Q + L_{AQ}(\dot{i}_q+\dot{i}_Q) \quad [pu] \qquad (2-9)$$

$$i_{od} = \frac{L_{AD}(\dot{i}_d+\dot{i}_F+\dot{i}_D) - \omega L_{AD}(i_F+i_Q)}{r_{e+h}} \quad [pu] \qquad (2-10)$$

$$i_{oq} = \frac{L_{AQ}(\dot{i}_q+\dot{i}_Q) + \omega L_{AD}(i_d+i_F+i_D)}{r_{e+h}} \quad [pu] \qquad (2-11)$$

Substituting eqs. (2-10) and (2-11) for eqs. (2-5), (2-8), these equations can conveniently be expressed in terms of machine currents and voltages. Finally, the equations are summarized as follows:

$$v = Ai + B\dot{i} - C\ddot{i} \quad [pu] \qquad (2-12)$$

where

$$v = [v_d \; v_F \; v_D \; v_q \; v_Q]^T$$

$$A = \begin{bmatrix} r - \frac{\omega^2\ell_q L_{AD}}{r_{e+h}} & -\frac{\omega^2\ell_q L_{AD}}{r_{e+h}} \\ 0 & r_F \\ 0 & 0 \\ \omega L_d + \frac{\omega r L_{AD} + \omega\ell_q L_{AD}}{r_{e+h}} & \omega L_{AD} + \frac{\omega r L_{AD} + \omega\ell_q L_{AD}}{r_{e+h}} \\ 0 & 0 \\ -\frac{\omega^2\ell_q L_{AD}}{r_{e+h}} & -\left(\omega L_q + \frac{\omega r L_{AQ} + \omega\ell_d L_{AQ}}{r_{e+h}}\right) \\ 0 & 0 \\ r_D & 0 \\ \omega L_{AD} + \frac{\omega r L_{AD} + \omega\ell_q L_{AD}}{r_{e+h}} & r - \frac{\omega^2\ell_d L_{AQ}}{r_{e+h}} \\ 0 & 0 \\ -\left(\omega L_{AQ} + \frac{\omega r L_{AQ} + \omega\ell_d L_{AD}}{r_{e+h}}\right) & \\ 0 & \\ 0 & \\ -\frac{\omega^2\ell_d L_{AQ}}{r_{e+h}} & \\ r_Q & \end{bmatrix}$$

$$B = \begin{bmatrix} L_d + \frac{rL_{AD}}{r_{e+h}} & L_{AD} + \frac{rL_{AD}}{r_{e+h}} \\ L_{AD} & L_F \\ L_{AD} & L_{AD} \\ \frac{\omega(\ell_d+\ell_q)L_{AD}}{r_{e+h}} & \frac{\omega(\ell_d+\ell_q)L_{AD}}{r_{e+h}} \\ 0 & 0 \\ L_{AD} + \frac{rL_{AD}}{r_{e+h}} & -\frac{\omega(\ell_d+\ell_q)L_{AQ}}{r_{e+h}} \\ L_{AD} & 0 \\ L_D & 0 \\ \frac{\omega(\ell_d+\ell_q)L_{AD}}{r_{e+h}} & L_q + \frac{rL_{AQ}}{r_{e+h}} \\ 0 & L_{AQ} \\ -\frac{\omega(\ell_d+\ell_q)L_{AQ}}{r_{e+h}} & \\ 0 & \\ 0 & \\ L_{AQ} + \frac{rL_{AQ}}{r_{e+h}} & \\ L_Q & \end{bmatrix}$$

$$C = \begin{bmatrix} \frac{\ell_d L_{AD}}{r_{e+h}} & \frac{\ell_d L_{AD}}{r_{e+h}} & \frac{\ell_d L_{AD}}{r_{e+h}} & 0 & 0 \\ 0 & 0 & 0 & 0 & 0 \\ 0 & 0 & 0 & 0 & 0 \\ 0 & 0 & 0 & \frac{\ell_q L_{AQ}}{r_{e+h}} & \frac{\ell_q L_{AQ}}{r_{e+h}} \\ 0 & 0 & 0 & 0 & 0 \end{bmatrix}$$

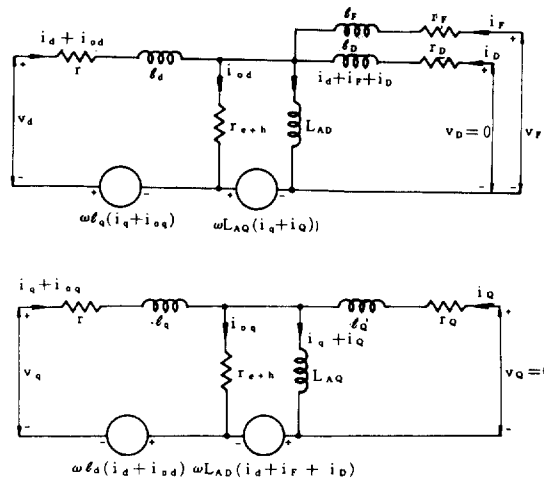

Fig. 2-2. New equivalent circuit.

where r_{e+h} is iron resistance, i_{od} d-axis iron current, i_{oq} q-axis iron current.

Ⅲ. CONTROL STRATEGIES.

In general, the air gap flux of an electric motor is maintained at, or near its nominal value for achieving a high utilization of motor iron for permitting the development of rated torque at all supply frequencies. For these reasons, the constant flux mode of control has been regarded as an optimum control strategy[23) 24)]. However, at light load, motor flux is greater than necessary for development of the required torque, and losses are high, resulting in a motor efficiency which is less than optimum. Otherwise, the air gap flux is excessively reduced, the armature currents and copper losses may rise unduly in developing the required torque at a specific speed. Consequently, there is an optimum set of armature input voltage, field excitation, and load angle combinations which gives the specified torque and speed with maximum efficiency. Accordingly, in order to develop the maximum efficiency condition, power input to a three-phase synchronous motor, under balanced and steady state conditions, from the new equivalent circuit model of Fig. 2-2 is:

$$P_i=[v_d(i_d+i_{od})+v_q(i_q+i_{oq})]/3+v_F i_F \text{(pu)} \tag{3-1}$$

where

$$\begin{bmatrix} v_d \\ v_q \end{bmatrix}=\sqrt{2/3}\begin{bmatrix} \cos\theta & \cos(\theta-2\pi/3) \\ -\sin\theta & -\sin(\theta-2\pi/3) \end{bmatrix}$$

$$\begin{bmatrix} \cos(\theta+2\pi/3) \\ -\sin(\theta+2\pi/3) \end{bmatrix}\begin{bmatrix} v_a \\ v_b \\ v_c \end{bmatrix}\text{[pu]}$$

$$\begin{bmatrix} i_d \\ i_q \\ i_F \end{bmatrix}=[T]^{-1}\begin{bmatrix} v_d \\ v_q \\ v_F \\ v_D=0 \\ v_Q=0 \end{bmatrix}\text{[pu]}$$

$$[T]=\begin{bmatrix} r-\dfrac{\omega^2\ell L_{AD}}{r_{e+h}} & -\left(\omega L_q+\dfrac{\omega r L_{AQ}}{r_{e+h}}\right) & -\dfrac{\omega^2\ell L_{AQ}}{r_{e+h}} & -\dfrac{\omega^2\ell L_{AD}}{r_{e+h}} \\ \omega L_d+\dfrac{\omega r L_{AD}}{r_{e+h}} & r-\dfrac{\omega^2\ell L_{AQ}}{r_{e+h}} & \omega L_{AD}+\dfrac{\omega r L_{AD}}{r_{e+h}} & \omega L_{AD}+\dfrac{\omega r L_{AD}}{r_{e+h}} \\ r_F & 0 & \omega L_{AD}+\dfrac{\omega r L_{AQ}}{r_{e+h}} & \\ & & -\dfrac{\omega^2\ell L_{AQ}}{r_{e+h}} & \\ & & 0 & \end{bmatrix}$$

$$v_F=r_F i_F\text{[pu]}$$

The correspondig electromagnetic torque is:

$$T_e=(\lambda_d i_q-\lambda_q i_d)/3\text{[pu]} \tag{3-2}$$

The power output, including windage and friction losses, is expressed as follows:

$$P_o=\omega_m T_e\text{[pu]} \tag{3-3}$$

where ω_m is synchonous angular velocity in mechanical radians per second. Optimal efficiency conditions (stationary conditions) may be derived from eqs. (3-1) and (3-3) at any specified torque (output power) and speed. Accordingly, the performance index for the problem is given by eq. (3-1). Since input power is expressed exclusively in terms of equivalent circuit parameters, with three variables: armature input voltage V, field excitation v_F, and load angle δ. The optimum efficiency value of the input power P_i subject to the constraint of eq. (3-3), is given by the function of three variables: V, v_F, and δ.

Define a H function as:

$$H(\beta,\ c)=P_i(\beta)+c^T P^o(\beta) \tag{3-4}$$

where

$c^T=[c_1\ c_2\cdots\cdots c_m]$: a set of constant multipliers.
$P^o(\beta)=\omega_m(\lambda_d i_q-\lambda_q i_d)/3-P_o$
$\beta=[V\ v_F\ \delta]$

The necessary and sufficient conditions for a minimum efficiency value of P_i are:

$$P^o(\beta)=0 \tag{3-5}$$
$$H(\beta,\ c)_\beta=0 \tag{3-6}$$

where

$$H(\beta, c)_{\beta} = (\partial H/\partial V \quad \partial H/\partial v_F \quad \partial H/\partial \delta)^T$$

Eqs. (3-5) and (3-6) are rewritten as :

$$\omega_m(\lambda_d i_q - \lambda_q i_d)/3 - P_o = 0 \qquad (3-7)$$

$$\partial H/\partial V = \partial H/\partial v_d \cdot \partial v_d/\partial V + \partial H/\partial v_q \cdot \partial v_q/\partial V = 0$$

$$\partial H/\partial v_F = 0$$

$$\partial H/\partial \delta = \partial H/\partial v_d \cdot \partial v_d/\partial \delta + \partial H/\partial v_q \cdot \partial v_q/\partial \delta = 0 \qquad (3-8)$$

Solution of eqs. (3-7) and (3-8) gives a stationary value of motor power input P_i. To determine the nature of the stationary value, it is necessary to investigate the behavior of second order differential changes in the H (β, c) function[26]. The second derivative matrix in the H(β, c) function is given by eq. (3-9), and a positive definite. Consequently, the stationary value obtained from eqs. (3-7) and (3-8) is an optimum value, V^*, v_F^*, and δ^*, which yields maximum efficiency at any specified torque and speed.

$$H(\beta, c)_{\beta\beta} = \begin{bmatrix} \partial^2 H/\partial V^2 & \partial^2 H/\partial V \partial v_F & \partial^2 H/\partial V \partial \delta \\ \partial^2 H/\partial v_F \partial V & \partial^2 H/\partial v_F^2 & \partial^2 H/\partial v_F \partial \delta \\ \partial^2 H/\partial \delta \partial V & \partial^2 H/\partial \delta \partial v_F & \partial^2 H/\partial \delta^2 \end{bmatrix} \qquad (3-9)$$

In addition, the flow chart which are used to solve the problem and the results are given in Fig. 3-1, and Table 3-1, respectively.

Table.3-1. Optimuum efficiency values for each load.

VARS / LDADS	V*[pu]	v_F*[pu]	δ*[°]
1/4RL	0.63	0.551	86.4
1/2RL	0.805	0.791	86.4
3/4RL	0.96	0.927	86.4
1R	0.998	0.99	86.4

The control loop for the practical realization of an efficiency-optimized synchonous motor drive is proposed in Fig. 3-2, and the flow chart for main and optimal efficiency tracking programs in Figs. 3-3 and 3-4, respectively. The proportional- integral (PI) controllers are used both current and speed controllers because of their easy turning and the absence of steady state error[25].

This control strategy can easily implemented by using an IBM personal computer.

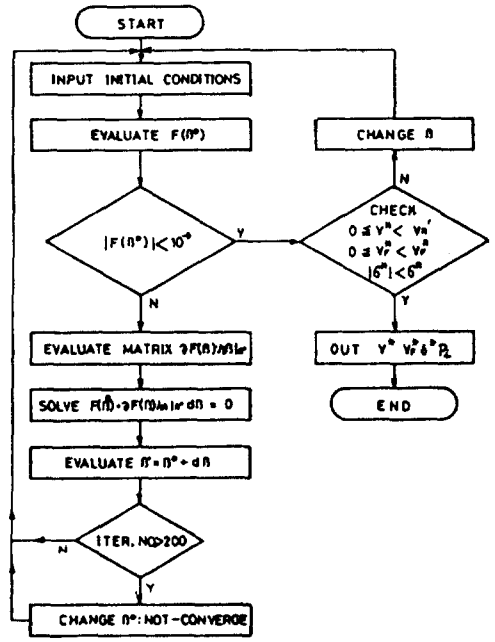

Fig. 3-1. Flow chart for obtaining optimum efficiency value.

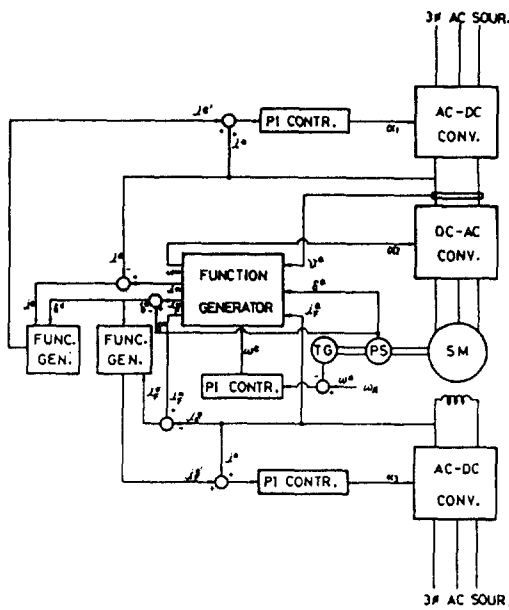

Fig. 3-2. Control loop for optimal efficiency control

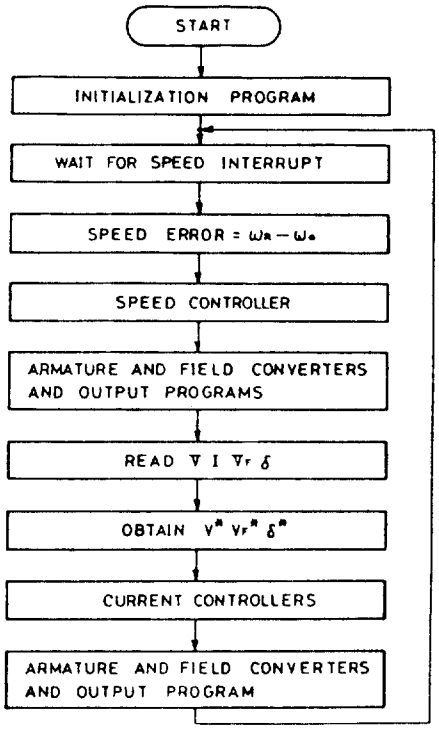

Fig. 3-3. Main flow chart.

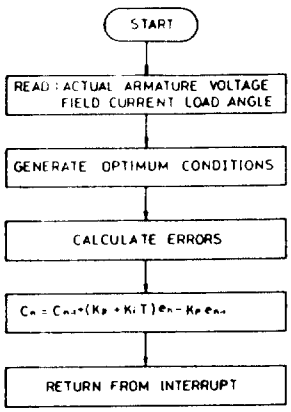

Fig. 3-4. Optimal efficiency tracking flow chart.

Also, since the non-sinusoidal supply to the motor causes additional harmonic losses, which must be taken into consideration when quantifying the efficiency improvement, and that sinusodial supply to the motor develops torque cogging, the optimum efficiency motor drive employs a revised McMurray voltage source inverter with an auxiliary commutation circuit,[27] as shown in Fig. 3-5. This generates a PAM waveform for establishing a good wave from including small harmonic contents of inverter output voltage.

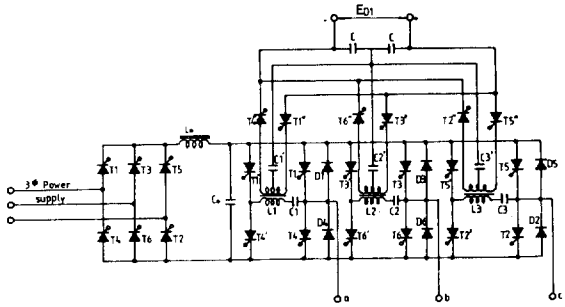

Fig. 3-5. Power circuit for synchronous motor drive.

Finally, the experimental results are shown in Fig. 3-6. The input power of the inverter is gradually decreased, the output is maintained constant, and the performance of the motor is carried to the most efficient state. To compare the efficiency of optimal operation (V/f: variable) with that of rated opperation (V/f: constant), the synchronous motor is driven under the rated operation for a while, and then the optimal efficiency control algorithm is applied. The output power is measured at the armature of dc dynamometer, the input power is measured at dc side of the inverter. If the efficiency of the inverter is considered to be constant, under the state at ¼, ½, ¾, or 1 of the rated output power with constant at 900 or 1800rpm, the input power is decreased through the range from 0.1% to 9.26%, respectively.

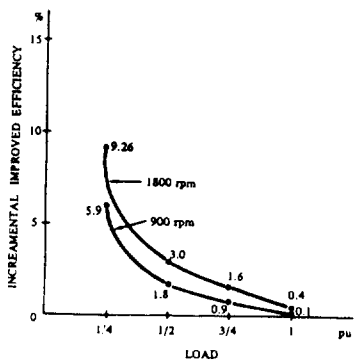

Fig. 3-6. Increamental efficiency improvement vs.each load.

Ⅳ. STABILITY STUDIES

During balanced and steady-state operations the rotor currents in damper windngs i_D and i_Q become zero and field current is constant. In this mode of operation, wherein the motor rotates at a constant speed, the time rate of change in rotor angle $s\varrho$ is a constant ω_0. The equations which describe balanced, steady state operation are expressed as:

$$v_{do}=V\cos\delta_o = r(i_{do}+i_{odo})+f_R L_{AQ} i_{qo} - f_R \ell_q (i_{qo}+i_{oqo}) \text{ (pu)} \quad (4-1)$$

$$v_{qo}=V\sin\delta_o = r(i_{qo}+i_{oqo})+f_R L_{AD}(i_{do}+i_{FO})+f_R \ell_d (i_{do}+i_{odo}) \text{ [pu]} \quad (4-2)$$

$$v_{FO}=r_F i_{FO} \text{ [pu]} \quad (4-3)$$

$$T_{eo}=[(L_d-L_q) i_{do} i_{qo} - kM_F i_{qo} i_{FO}]/3 \text{ [pu]} \quad (4-4)$$

where the subscript o has been added so as to denote steady state quantities. The steady state rotor angle δ_o and the frequency ratio f_R, and the steady state iron currents i_{odo}, i_{oqo}, are defined as:

$$\delta_o=\theta-\omega_o t-\pi/2 \quad (4-5)$$

$$f_R=\omega_o/\omega_B \quad (4-6)$$

$$i_{odo}=-\omega_o L_{AQ} i_{qo}/r_{e\cdot h} \quad (4-7)$$

$$i_{oqo}=\omega_o L_{AD}(i_{do}+i_{FO})/r_{e\cdot h} \quad (4-8)$$

It is clear that frequency ratio f_R depends upon the value of electrical angular velocity of the applied stator voltages and f_R is unity when this angular velocity equals ω_B. If all variables are permitted to change by a small amount about an initial operating point, eq. (2-12) becomes, in matrix form

$$\begin{bmatrix} -\sqrt{3}V\sin(\delta_o+\triangle\delta) \\ v_{FO} \\ 0 \\ -\sqrt{3}V\cos(\delta_o+\triangle\delta) \\ 0 \end{bmatrix} = \begin{bmatrix} A_{11} & A_{12} & A_{13} & A_{14} & A_{15} \\ A_{21} & A_{22} & A_{23} & A_{24} & A_{25} \\ A_{31} & A_{32} & A_{33} & A_{34} & A_{35} \\ A_{41} & A_{42} & A_{43} & A_{44} & A_{45} \\ A_{51} & A_{52} & A_{53} & A_{54} & A_{55} \end{bmatrix} \begin{bmatrix} i_{do}+i_d \\ i_{FO}+i_F \\ \triangle i_D \\ i_{qo}+i_q \\ \triangle i_Q \end{bmatrix} \quad (4-9)$$

where

$$A_{11}=r-\frac{\left(f_R+\frac{\triangle\omega}{\omega}\right)^2 \ell_q L_{AD}}{r_{e\cdot h}}+\left(L_d+\frac{rL_{AD}}{r_{e\cdot h}}\right)s + \frac{\ell_d L_{AD}}{r_{e\cdot h}}s^2$$

$$A_{12}=-\frac{\left(f_R+\frac{\triangle\omega}{\omega}\right)^2 \ell_q L_{AD}}{r_{e\cdot h}}+\left(L_{AD}+\frac{rL_{AD}}{r_{e\cdot h}}\right)s + \frac{\ell_d L_{AD}}{r_{e\cdot h}}s^2$$

$$A_{13}=A_{12}$$

$$A_{14}=-\left(f_R+\frac{\triangle\omega}{\omega}\right)L_q - \frac{\left(f_R+\frac{\triangle\omega}{\omega}\right)rL_{AQ}+s\left(f_R+\frac{\triangle\omega}{\omega}\right)\ell_d L_{AQ}}{r_{e\cdot h}} - \frac{\left(f_R+\frac{\triangle\omega}{\omega}\right)(\ell_d+\ell_q)L_{AQ}}{r_{e\cdot h}}s$$

$$A_{15}=-\left(f_R+\frac{\triangle\omega}{\omega}\right)L_{AQ} - \frac{\left(f_R+\frac{\triangle\omega}{\omega}\right)rL_{AQ}+s\left(f_R+\frac{\triangle\omega}{\omega}\right)\ell_d L_{AQ}}{r_{e\cdot h}} - \frac{\left(f_R+\frac{\triangle\omega}{\omega}\right)(\ell_d+\ell_q)L_{AQ}}{r_{e\cdot h}}s$$

$$A_{21}=sL_{AD}$$

$$A_{22}=r_F+sL_F$$

$$A_{23}=A_{21}$$

$$A_{24}=0$$

$$A_{25}=0$$

$$A_{31}=sL_{AD}$$

$$A_{32}=A_{31}$$

$$A_{33}=r_D+sL_D$$

$$A_{34}=0$$

$$A_{35}=0$$

$$A_{41}=\left(f_R+\frac{\triangle\omega}{\omega}\right)L_d + \frac{\left(f_R+\frac{\triangle\omega}{\omega}\right)rL_{AD}+s\left(f_R-\frac{\triangle\omega}{\omega}\right)\ell_q L_{AD}}{r_{e\cdot h}} + \frac{\left(f_R+\frac{\triangle\omega}{\omega}\right)(\ell_d+\ell_q)L_{AD}}{r_{e\cdot h}}s+\frac{\ell_d L_{AD}}{r_{e\cdot h}}s^2$$

$$A_{42}=\left(f_R+\frac{\triangle\omega}{\omega}\right)L_{AD} + \frac{\left(f_R+\frac{\triangle\omega}{\omega}\right)rL_{AD}+s\left(f_R+\frac{\triangle\omega}{\omega}\right)\ell_q L_{AD}}{r_{e\cdot h}}$$

$$+\frac{\left(f_R+\frac{\triangle\omega}{\omega}\right)(\ell_d+\ell_q)L_{AD}}{r_{e\cdot h}}s+\frac{\ell_d L_{AD}}{r_{e\cdot h}}s^2$$

$$A_{43}=A_{42}$$

$$A_{44}=r-\frac{\left(f_R+\frac{\triangle\omega}{\omega}\right)^2\ell_d L_{AQ}}{r_{e\cdot h}}+\left(L_Q+\frac{rL_{AQ}}{r_{e\cdot h}}\right)s+\frac{\ell_q L_{AQ}}{r_{e\cdot h}}s^2$$

$$A_{45}=-\frac{\left(f_R+\frac{\triangle\omega}{\omega}\right)^2\ell_d L_{AQ}}{r_{e\cdot h}}+\left(L_{AQ}+\frac{rL_{AQ}}{r_{e\cdot h}}\right)s+\frac{\ell_q L_{AQ}}{r_{e\cdot h}}s^2$$

$$A_{51}=0$$

$$A_{52}=0$$

$$A_{53}=0$$

$$A_{54}=sL_{AQ}$$

$$A_{55}=r_Q+sL_Q$$

Using the approximation

$$V\cos(\delta_o+\triangle\delta)=V\cos\delta_o-V\sin\delta_o\triangle\delta \qquad (4-10)$$

$$V\sin(\delta_o+\triangle\delta)=V\sin\delta_o-V\cos\delta_o\triangle\delta \qquad (4-11)$$

and eliminating the steady-state terms defined by eqs. (4-1)-(4-4), the previous matrix equation can be solved for the quantities only. The resulting set of linear differential equation is:

$$\begin{bmatrix}\sqrt{3}V\cos\delta_o\triangle\delta+a_1i_{do}+b_1i_{Fo}+c_1i_{qo}\\0\\0\\-(-\sqrt{3}V\sin\delta_o\triangle\delta+a_2i_{do}+b_2i_{Fo}+c_2i_{qo})\\0\end{bmatrix}$$

$$=\begin{bmatrix}B_{11}&B_{12}&B_{13}&B_{14}&B_{15}\\B_{21}&B_{22}&B_{23}&B_{24}&B_{25}\\B_{31}&B_{32}&B_{33}&B_{34}&B_{35}\\B_{41}&B_{42}&B_{43}&B_{44}&B_{45}\\B_{51}&B_{52}&B_{53}&B_{54}&B_{55}\end{bmatrix}\begin{bmatrix}\triangle i_d\\\triangle i_F\\\triangle i_D\\\triangle i_q\\\triangle i_Q\end{bmatrix} \qquad (4-12)$$

where

$$a_1=\frac{2f_R\ell_q L_{AD}s\triangle\delta/\omega}{r_{e\cdot h}}$$

$$b_1=a_1$$

$$c_1=L_q s\triangle\delta/\omega+\frac{rL_{AQ}s\triangle\delta/\omega+\ell_q L_{AQ}s^2\triangle\delta/\omega}{r_{e\cdot h}}$$

$$a_2=L_d s\triangle\delta/\omega+\frac{rL_{AD}s\triangle\delta/\omega+\ell_q L_{AD}s^2\triangle\delta/\omega}{r_{e\cdot h}}$$

$$b_2=L_{AD}s\triangle\delta/\omega+\frac{rL_{AD}s\triangle\delta/\omega+\ell_q L_{AD}s^2\triangle\delta/\omega}{r_{e\cdot h}}$$

$$c_2=\frac{2f_R\ell_d L_{AQ}s\triangle\delta/\omega}{r_{e\cdot h}}$$

$$B_{11}=r-\frac{\omega^2\ell_q L_{AD}}{r_{e\cdot h}}+\left(L_d+\frac{rL_{AD}}{r_{e\cdot h}}\right)s+\frac{\ell_d L_{AD}}{r_{e\cdot h}}s^2$$

$$B_{12}=-\frac{\omega^2\ell_q L_{AD}}{r_{e\cdot h}}+\left(L_{AD}+\frac{rL_{AD}}{r_{e\cdot h}}\right)s+\frac{\ell_d L_{AD}}{r_{e\cdot h}}s^2$$

$$B_{13}=B_{12}$$

$$B_{14}=-\left(\omega L_q+\frac{\omega rL_{AQ}+s\omega\ell_d L_{AQ}}{r_{e\cdot h}}\right)-\frac{\omega(\ell_q+\ell_d)L_{AQ}}{r_{e\cdot h}}s$$

$$B_{15}=-\left(\omega L_{AQ}+\frac{\omega rL_{AQ}+s\omega\ell_d L_{AQ}}{r_{e\cdot h}}\right)-\frac{\omega(\ell_q+\ell_d)L_{AQ}}{r_{e\cdot h}}s$$

$$B_{21}=sL_{AD}$$

$$B_{22}=r_F+sL_F$$

$$B_{23}=B_{21}$$

$$B_{24}=0$$

$$B_{25}=0$$

$$B_{31}=sL_{AD}$$

$$B_{32}=B_{31}$$

$$B_{33}=r_D+sL_D$$

$$B_{34}=0$$

$$B_{35}=0$$

$$D_{41}=\omega L_d+\frac{\omega rL_{AD}+s\omega\ell_q L_{AD}}{r_{e\cdot h}}+\frac{\omega(\ell_q+\ell_d)L_{AD}}{r_{e\cdot h}}s$$

$$B_{42}=\omega L_{AD}+\frac{\omega rL_{AD}+s\omega\ell_q L_{AD}}{r_{e\cdot h}}+\frac{\omega(\ell_q+\ell_d)L_{AD}}{r_{e\cdot h}}s$$

$$B_{43}=B_{42}$$

$$B_{44}=r-\frac{\omega^2\ell_d L_{AQ}}{r_{e\cdot h}}+\left(L_Q+\frac{rL_{AQ}}{r_{e\cdot h}}\right)s+\frac{\ell_q L_{AQ}}{r_{e\cdot h}}s^2$$

$$B_{45}=-\frac{\omega^2\ell_d L_{AQ}}{r_{e\cdot h}}+\left(L_q+\frac{rL_{AQ}}{r_{e\cdot h}}\right)s+\frac{\ell_q L_{AQ}}{r_{e\cdot h}}s^2$$

$$B_{41}=0$$

$$B_{52}=0$$

$$B_{53}=0$$

$$B_{54}=sL_{AQ}$$

$$B_{55}=r_Q+sL_Q$$

The linearized torque equation valid for small variations about an operating point is:

$$\triangle T_e=T_e-T_{eo}=[(L_d(i_{do}+\triangle i_d)+kM_F(i_{Fo}+\triangle i_F)+kM_D\triangle i_D)(i_{qo}+\triangle i_q)-(L_q(i_{qo}+\triangle i_q)-kM_Q\triangle i_Q)(i_{do}+\triangle i_d)-(L_d i_{do}+kM_F i_{Fo})i_{qo}+(L_q i_{qo}i_{do})]/3 \qquad (4-13)$$

It is evident from the form of eq. (4-12) that the three rotor currents can be expressed in terms of the stator currents. If the resulting 2×2 matrix is solved for $\triangle i_d$ and $\triangle i_q$ in terms of $\triangle\delta$ and the results substituted into eq. (4-13), it is clear that one can obtain an expression which has the form:

$$\triangle T_e = G(s)\triangle\delta \qquad (4-14)$$

The expression for the transfer function G(s) is included in Appendix B. In order to completely describe the behavior of the motor about a steady-state operating point, dynamicsof the mechanical system must be considered. In steady state, load torque T_{m0} is equal to electromangnetic torque T_{e0}. If $\triangle T_m$ is a small value in eq. (3-3), positive change from steady state load torque then:

$$T_{mo}+\triangle T_m = T_{eo}+\triangle T_e - \frac{1}{\omega_B}(2Hs^2\triangle\delta + Ds\triangle\delta) \qquad (4-15)$$

Eluminating the steady state terms yields

$$\triangle T_m = \triangle T_e - \frac{1}{\omega_B}(2Hs^2\triangle\delta + Ds\triangle\delta) \qquad (4-16)$$

Eqs. (4-14) and (4-16) suggest the block diagram representation shown in Fig. 4-1. By employing the method of small displacements, the problem of determining synchronous motor stability has been recast in the form of a simple feedback control system. Consequently, the problem of motor stability is amenable to any of the approaches commonly employed in linear feedback control theory. Stability could be established employing the Routh test or the root locus method; however, a Nyquist criterion will be used in this development. It is clear from Fig. 4-1 that the open loop transfer function is:

$$F(s) = \frac{\omega_B G(s)}{2Hs^2+Ds} \qquad (4-17)$$

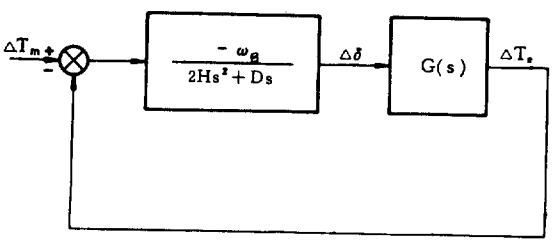

Fig. 4-1. Small displacement & closed loop system.

The stability of the closed loop system can be determined by setting $s=j\nu$ and observing the locus of $F(j\nu)$ as ν varies from $-\infty$ to $+\infty$. Since F(s) does not have poles with positive real parts, the closed loop system is stable if, and only if, the locus of $F(j\nu)$ does not pass through or encircle the (-1,0) point. The equations which have been developed offer a convenient means of predicting the behavior of a synchronous motor. A change in frequency is taken into account by a change in the value of f_R. Throughout this study, 60 Hz is assumed to be the rated frequency and the per unit system employed is based on operation at this frequency. Thus, the frequency ratio f_R can be interpreted as the steady state operating speed expressed per unit. By utilizing previous equations already developed, a digital computer can easily be programmed to compute Nyquist contours for the entire range of possible operating conditions in a manner similar to that carried out for the reluctance synchronous machine[26]. If the particular motor studied in unstable, the region of instability can readily be determined. A region of instability for a three-phase, four-pole, 7.5 hp, and 60 Hz synchronous motor is shown in Figs. 4-2, 4-3. The per unit parameters of the motor corresponding to these results are presented in Appendix A. In Figs. 4-2 and 4-3, the amplitude of applied armature voltages decreases in linear form with frequency. That is to say:

$$v = f_R V \qquad (4-18)$$

The field voltage v_F defined as the per unit is expressed as

$$V_F = \frac{\omega L_{AD} V_F}{r_F} \qquad (4-19)$$

With the motor operating at base or unit speed, unit voltage is induced in the stator (armature) winding if V_F is unity. Fig. 4-2, V_F is fixed at 1.0 per unit. The dashed line shown in Figs. 4-2 and 4-3 indicates the pull out or maximum steady state torque at various operating speeds. The closed contour forms the boundary between stable and unstable regions of operation. The contours shown in Fig. 4-2 ilustrate that stability of this same motor is improved as a result of an increase in the amplitude of the stator applied voltages. In all cases applied stator voltage v experiences linear decrease with f_R. that is $v=f_R V$, where the voltage V is normally 1.0

per unit. Fig. 4-2 shows the contours for V=1.0, 1.1, and 1.2 per unit. The increase in the region of instability due to an increase in field excitation is shown in Fig. 4-3. Contours are given for V_F=0.75, 1.0, and 1.25 per unit. It is noted that an increase in terminal voltage serves to stabilize the motor whereas an increase in field excitation tends to make the motor less stable. Also, the instability regions for load changes are shown in Fig. 4-4.

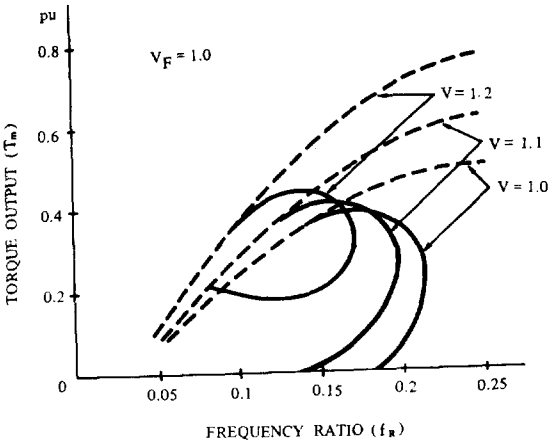

Fig. 4-2. Instability regions for armature input voltages.

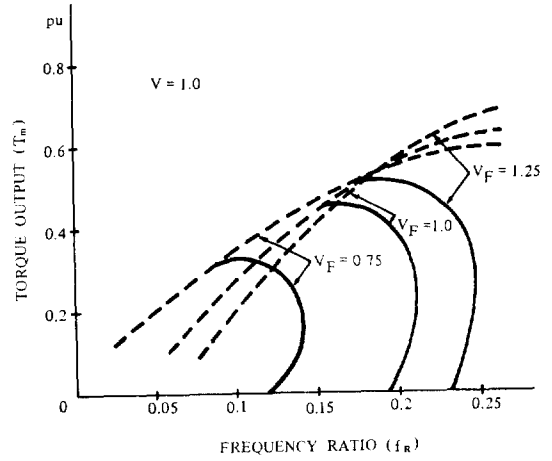

Fig. 4-3. Instability regions for field excitations.

V. CONCLUSIONS

In order to study the accurate performance and characteristics of a synchonous motor at maximum efficiency, a comprehensive equivalent circuit model of the motor

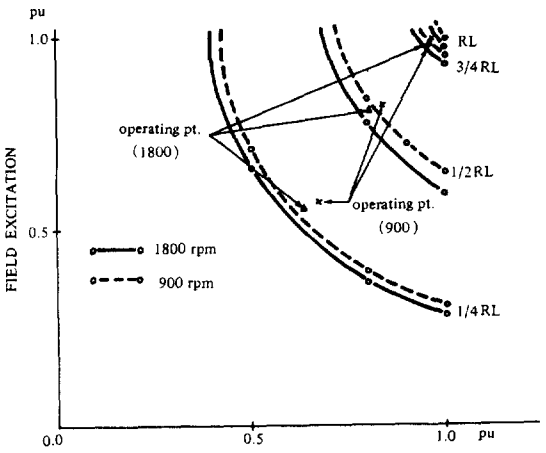

Fig. 4-4. Instability regions for loads.

was developed incorporating the frequency dependent nature of its parameters and the effects of iron loss. From the equivalent circuit model, a characteristic equation related to motor input and output was derived, and then, optimum efficiency conditions were established by applying Lagrange multiplier theory to the equation stable regions over the whole range of loads.

These conditions were met by the of a PAM inverter as a power circuit for minimum harmonic effects and easy control, and a 16-bit microcomputer as control loop for real time control.

During maximum efficiency operation, the motor is found to be stable when the Nyquist stability criterion is applied to the linearized equations which describe the behavior of the motor when the motor loads perturb about a steady-state operating point.

Based on the work reported in this dissertation, the following conclusions are arrived at:

1. Optimal efficiency conditions as the combinations of armature voltage, field excitation, and load angle are invariably present in stable regions over the whole range of loads.
2. Power saving is possible in all load conditions, particularly remarkable saving accuring at light loads.
3. Motor efficiency improves as speed increases.
4. In maximum efficiency operations, load angle maintains a constant value (86.4 degrees) regardless of load conditions.
5. In maximum efficiency operations, a good power factor (over 0.8) prevails under any load conditions.

6. Despite the reduction of the motor air-gap flux in maximum efficiency conditions, the motor driven system is usually stable, But a sudden great change of the motor load makes normal operation impossible.
7. Motor stability improves by increasing armature voltage or decreasing field excitation.

When major components required for this system and the standardized micro processors for controlling the motor have begun to be commercially produced the control system designed for maximum- efficiency operation of the motor could be manufactured and installed at much low costs. This will promote wider utilization of the system and be instrumental in energy saving.

Finally, thank the authorities of the Ministry of Education about financial support for this paper.

REFERENCE

1) J.C. Andreas, Energy Efficient Electric Motors, Marcel Dekker, 1982.
2) N. Mohan, "Improvement in Energy Efficiency of Induction Motors by means of Voltage Control," IEEE Trans PAS., Vol. PAS-99, No. 4, July / Aug., 1980.
3) J. Hindmarsh, Electrical Machines and Their Applications, Pergamon, 1977.
4) A. Mychael, AC Machines, McGraw-Hill, 1977.
5) A.E. Fitzgerald, et. al., Electric Machinery, McGraw-Hill, 1971.
6) G.R. Slemon, Magnetoelectric Devices, Wiley, 1966.
7) L.W. Matsch, Electromagnetic & Electromechanical Machines, IEP, 1977.
8) E. Levi, et. al., Electromechanical Power Conversion, Dover, 1974.
9) G.R. Slemon, et. al., Electric Machines, Addison-Wesley, 1980.
10) C.T.A. Johnk, Engineering Electromagnetic Fields & Waves, Wiley, 1975.
11) D.S. Hyun, et. al., "Synchronous Motor Operation with Maximum Efficiency," Univ. of Toledo, OH., 1985.
12) J.M.D. Murphy, et. al., "Efficiency Optimization of Inverter Fed Induction Motor Drives," IEEE IAS Annu. Meeting, 1982.
13) M.H. Park, et. al., "Optimal Efficiency Drive of a Current Source Inverter Fed Induction Motor by Flux Control," IEEE Trans. IA., Vol. IA-20, No. 6, p. 1453-59, Novv. / Dec., 1984.
14) J.C. Prescott, et. al., "The Inherent Instability of Synchronous Machinery," J.IEE, Vol. 75, p. 497-511, 1984.
15) A.P. Sage, et. al., Optimum Systems Control, Library of Congress, 1977.
16) B.C. Kuo, Automatic Control Systems, Prentice-Hall, 1982.
17) T.A. Lipo, et. al., "Stability Analysis for Variable Frequency Operation of Synchronous Machines," IEEE Trans. PAS., Vol. PAS-97, No. 1, p. 227-34, Jan., 1968.
18) D.W. Novotny, et. al., "Theoretical and Experimental Analysis of Operating Point Stability of Synchronous Machines," IEEE PAS. Summer Meeting, 1970.
19) Y. Yu, et. al., "Experimental Determination of Exact Equivalent Circuit Parameters of Synchronous Machines," IEEE Winter Power Meeting, 1971.
20) M. Riaz, "Hybrid Parameter Models of Synchronous Machines," IEEE IA. Ann. Meeting, 1973.
21) P. M. Anderson, et. al., Power System Control and Stability, the IOWA STATE Univ. PRESS, AMES, IOWA, U.S.A.
22) M.H. Park, et. al., "New Equivalent Circuit of a Synchronous Machine," KIEE, Vol. 34, No. 11, p. 20-24, Nov., 1985.
23) A. Bellini, et. al., "Voltage-Frequency Law in Frequency Controlled Induction Motor Drives," IEEE IA 13th Annu. Meeting, 1978.
24) G. Danzing et. al., "Optimum: Konstanter Fluss," Electrotechnik,Vol. 61, No. 21, p. 24-27, Nov., 1979.
25) M.H. Park, et. al., "Microprocessor- Based Optimal Efficiency Drive of an Induction Motor," IEEE Trans. IE, Vol. IE-31, No. 1, Feb., 1984.
26) A.E. Bryson, et. al., Applied Optimal Control, Walthan, 1969.
27) D.S. Hyun, "optimal Efficiency Control of a Synchronous Motor," Ph.D. dissertation, Seoul National University, 1986.

APPENDIX A

SYNCHRONOUS MOTOR RATINGS AND PARAMETERS

3-phase 4-pole 7.5 hp

Rated armature voltage	240 V
Rated armature current	13.5 A
Rated field voltage	135 V
Rated field current	2.1 A
Rated speed	1800 rpm
Frequency	60 Hz
Power factor	0.8 pf

$r=0.04157$ pu $\quad r_F=0.002668$ pu $\quad r_D=0.031177$ pu
$r_Q=0.132$ pu $\quad r_{e+h}=11.2034$ pu
$L_d=0.72945$ pu $\quad L_q=0.4508$ pu $\quad L_F=0.6824$ pu
$L_D=0.63918$ pu $\quad L_Q=0.35734$ pu $\quad l_d=l_q=0.11345$ pu
$L_{AD}=0.616$ pu $\quad L_{AQ}=0.3373$ pu
$H=1.721485$s $\quad \tau_1=1297.312 \quad D=0.05637$ pu

APPENDIX B

SYSTEM TRANSFER FUNCTION

$$Z_1=r-\frac{\omega^2 l_d L_{AQ}}{r_{e+h}}+s\left(L_q+\frac{rL_{AQ}}{r_{e+h}}\right)+s^2\frac{l_q L_{AQ}}{r_{e+h}}-\frac{\left\{\frac{-\omega^2 l_d L_{AQ}}{r_{e+h}}+s\left(L_{AQ}+\frac{rL_{AQ}}{r_{e+h}}\right)+s^2\frac{l_q L_{AQ}}{r_{e+h}}\right\}^2}{r_D+sL_D}$$

$$Z_2=\omega L_d+\frac{\omega rL_{AD}+s\omega l_q L_{AD}}{r_{e+h}}+s\frac{\omega(l_d+l_q)L_{AD}}{r_{e+h}}-\left\{\omega L_{AD}+\frac{\omega rL_{AD}+s\omega l_q L_{AD}}{r_{e+h}}+s\frac{\omega(l_d+l_q)L_{AD}}{r_{e+h}}\right\}\cdot\left\{-\frac{\omega^2 l_q L_{AD}}{r_{e+h}}+s\left(L_{AD}+\frac{rL_{AD}}{r_{e+h}}\right)+s^2\frac{l_d L_{AD}}{r_{e+h}}\right\}\cdot\{r_F+r_D+s(L_F+L_D-2L_{AD})\}/[\{r_D+s(L_D-L_{AD})\}\{r_F+sL_F\}+\{r_F+s(L_F-L_{AD})\}\{sL_{AD}\}]$$

$$Z_3=-\frac{\omega^2 l_q L_{AD}}{r_{e+h}}+s\left(L_{AD}+\frac{rL_{AD}}{r_{e+h}}\right)+s^2\frac{l_d L_{AD}}{r_{e+h}}+\left\{\omega L_{AQ}+\frac{\omega r_{AQ}+s\omega l_d L_{AQ}}{r_{e+h}}+s\frac{\omega(l_d+l_q)L_{AQ}}{r_{e+h}}\right\}\cdot\left\{-\frac{\omega^2 l_d L_{AQ}}{r_{e+h}}+s\left(L_{AQ}+\frac{rL_{AQ}}{r_{e+h}}\right)+s^2\frac{l_q L_{AQ}}{r_{e+h}}\right\}/(r_Q+sL_Q)$$

$$Z_4=r-\frac{\omega^2 l_q L_{AD}}{r_{e+h}}+s\left(L_d+\frac{rL_{AD}}{r_{e+h}}\right)+s^2\frac{l_d L_{AD}}{r_{e+h}}-\frac{s^2(L_{AD})^2\{r_F+r_D+s(L_F+L_D-2L_{AD})\}}{\{r_D+s(L_D-L_{AD})\}\{(r_F+sL_F)\{r_F+s(L_{AD})\}sL_{AD}}$$

$$V_1=-\left\{-\sqrt{3}V\sin\delta_0+\frac{s}{\omega}L_d i_{d0}+\frac{srL_{AD}+s^2 l_q L_{AD}}{\omega r_{e+h}}i_{d0}+\frac{s}{\omega}L_{AD}i_{F0}+\frac{srL_{AD}+s^2 l_q L_{AD}}{\omega r_{e+h}}i_{F0}-\frac{2sf_R l_d L_{AQ} i_{q0}}{\omega r_{e+h}}\right\}$$

$$V_2=\sqrt{3}V\cos\delta_0+\frac{2sf_R l_q L_{AD}}{\omega r_{e+h}}i_{d0}+\frac{2sf_R l_q L_{AD}}{\omega r_{e+h}}i_{F0}+\frac{sL_q}{\omega}i_{q0}+\frac{srL_{AQ}+s^2 l_q L_{AQ}}{\omega r_{e+h}}$$

$$V_3=\omega(L_d-L_q)i_{d0}+\omega L_{AD}i_{F0}+\frac{s^2 L_{AQ}^2 i_{d0}}{r_Q+sL_Q}$$

$$V_4=\omega(L_d-L_q)i_{q0}+\omega L_{AD}i_{q0}-\frac{sL_{AD}^2 i_{q0}\{r_F+r_D+s(L_F+L_D-2L_{AD})\}}{(r_F+sL_F)(r_D+sL_D)-s^2L_{AD})^2}$$

$$G(s)=\frac{(V_1Z_4-V_2Z_2)V_3}{Z_1Z_4-Z_2Z_3}+\frac{(V_2Z_1-V_1Z_3)V_4}{Z_1Z_4-Z_2Z_3}$$